Available online at www.sciencedirect.com
ScienceDirect
Physics Letters A 372 (2007) 72–76
PHYSICS LETTERS A
www.elsevier.com/locate/pla

Electronic and optical properties of ZnO thin film under in-plane biaxial strains: Ab initio calculation

Y.Q. Gai [a,b,*], B. Yao [a,c], Y.M. Lu [a], D.Z. Shen [a], J.Y. Zhang [a], D.X. Zhao [a], X.W. Fan [a]

[a] *Key Laboratory of Excited State Processes, Changchun Institute of Optics, Fine Mechanics and Physics, Chinese Academy of Science, Changchun 130033, People's Republic of China*
[b] *Graduate School of the Chinese Academy of Sciences, Beijing 100049, People's Republic of China*
[c] *National Laboratory of Superhard Materials, Jilin University, Changchun 130012, People's Republic of China*

Received 30 May 2007; received in revised form 26 June 2007; accepted 2 July 2007

Available online 5 July 2007

Communicated by J. Flouquet

Abstract

The full regions of the electronic and optical properties of in-plane biaxial strained thin film ZnO are studied using pseudopotential plane-wave method. The fundamental band gap at the Γ point increase linearly with the increase of tensile strains, but decreased with the compressive ones. The strains affected the local tetrahedral symmetry, and so the splitting of crystal field energy. The band dispersion relation of the valence band maximum changes with the strains, which means the residual strains have effects on the effective hole mass, thus the transportation properties of the p-type ZnO. The changes tendency of optical properties up to full regions under strains have been shown and discussed.
© 2007 Elsevier B.V. All rights reserved.

1. Introduction

Zinc oxide is an II–VI group wide band gap semiconductor and an attractive multi-functional material because of its applications to short-wavelength emitting diodes, photo detectors, UV nanolaser, and electroluminescence devices [1,2]. A great deal of efforts has been made on ZnO epitaxy layers grown various substrates, such as α-Al_2O_3 [3], 6H-SiC [4], Si [5], GaAs [6] and $ScAlMgO_4$ [7], etc. The lattice mismatch between the substrate and the deposited layer as well as the difference in the thermal expansion coefficients between them always induce residual strain in the heteroepitaxial layers, which has to be taken into account in order to grow high quality thin ZnO films. It is well known that the energy of the conduction band minimum (CBM) and valence band maximum (VBM) of the wurtzite semiconductors can be altered via hydrostatic pressures [8], or alloying [9] through changing their lattice constants, so will do the residual strains. These strain effects have been, for example, intensely investigated over the past ten years in the case of GaN-based layers [10–14], which all revealed that the residual strains had much effect on its electrical and optical properties. Recently such experimentally works have been done on ZnO-based heterostructures [16,17]. However theoretical study is almost completely missing. In this work, we carried out band-structure and optical properties calculations for ZnO under varying degrees of in-plane biaxial strains, induced by mismatch and defects.

2. Method

The ab initio calculations described here are performed with the CASTEP code [18], based on density functional theory (DFT) using pseudo-potentials to describe the electron–ion interactions and a plane-wave to expand the waves functions. We use the generalized gradient approximation (GGA) in the

* Corresponding author at: Key Laboratory of Excited State Processes, Changchun Institute of Optics, Fine Mechanics and Physics, Chinese Academy of Science, Changchun 130033, People's Republic of China.
E-mail address: xiaogaijiaping@sohu.com (Y.Q. Gai).

0375-9601/$ – see front matter © 2007 Elsevier B.V. All rights reserved.
doi:10.1016/j.physleta.2007.07.001

scheme of Perdew–Burke–Eruzerhof (PBE) to describe the exchange and correlation potential, since the GGA is relatively more efficient to predict the energy gap of semiconductor than the local-density approximation (LDA) [19], which is well known to underestimate the fundamental band gap in semiconductors and insulators by 30–60% [20], but the shape of the bands is usually in agreement with results from band structure calculations which go beyond the DFT-LDA. In the calculation of electronic properties, we used Vanderbilt-type ultrasoft pseudopotential [21] which allows calculations to be performed with the lowest possible cutoff energy for the plane-wave basis set and used norm-conserving pseudopotentials [22] for optical properties calculations. Brillouin zone integrations were performed using a Monkhorst–Pack sampling scheme. We have Zn $3d^{10}4s^2$ and O $2p^6$ as the valence electrons and carefully investigated the dependences of the total energy on the cutoff energy and the k-point set mesh so as to make our results reasonable. Finally, the valence electron wave functions were expanded in a plane-wave basis set up to a kinetic energy cutoff of 700 eV. This converges total energy differences to better than 1 meV/atom. A $9 \times 9 \times 6$ Monkhorst–Pack grid was used, leading to 36 k-points in the irreducible Brillouin zone for the high symmetry structure, which make the separation of the reciprocal space to be less than 0.03 Å^{-1}. In order to compensate the GGA underestimation of the band gap, the calculated optical spectra have been shifted by the scissors operator, which is a rigid shift of the conduction bands with respect to the valence bands in order to match the experimental band gap of ZnO.

When it comes to the in-plane strains, we applied the method used in Ref. [23]. The space-group symmetry of the wurtzite structure C_{6v}^4 is conserved, and strain and stress tensors take diagonal form as

$$\varepsilon_{xx} = \varepsilon_{yy} = (a - a_0)/a_0 \quad \text{and} \tag{1a}$$

$$\varepsilon_{zz} = (c - c_0)/c_0. \tag{1b}$$

Here, a_0 (a) and c_0 (c) denote the lattice constants of the unstrained (strained) crystal, and the convention is used that $\varepsilon_{xx} < 0$ ($\varepsilon_{xx} > 0$) for layers under compressive (tensile) in-plane strain. In the limit of small deviations from the equilibrium, the corresponding stress tensor components follow according to Hooke's law,

$$\sigma_{xx} = (C_{11} + C_{12})\varepsilon_{xx} + C_{13}\varepsilon_{zz} \quad \text{and} \tag{2a}$$

$$\sigma_{zz} = 2C_{13}\varepsilon_{xx} + C_{33}\varepsilon_{zz}. \tag{2b}$$

Where the parameters C_{ij} denote the elastic constants. In Eqs. (2) four of the five independent constants C_{ij} of the considered wurtzite crystal occurs. A homogeneous biaxial stress in the plane perpendicular to the c axis of the wurtzite lattice is described by constant forces in this plane, $\sigma_{xx} = \sigma_{yy}$, and the forces along the c axis, $\sigma_{zz} = 0$. Then Eqs. (2) gives a relationship between the strain components, $\varepsilon_{zz} = -R^B \varepsilon_{xx}$, with the coefficient $R^B = 2C_{13}/C_{33}$, which means that the tensile biaxial strain in the ab plane results in compressive uniaxial strain along the c-axis [15]. In order to determine the biaxial relaxation coefficient R^B, we choose lattice constants a close to the equilibrium one and, in each case, minimize the total energy of the system with respect to the second lattice constant c and the internal parameter u to obtain the relaxed value of c.

3. Results

3.1. The electronic properties under strains

The effects of biaxial strains are considered both on microscopic scales, i.e., on the internal cell parameter u ($= d/c$), where d refers to the Zn–O bond length along the c-axis, and on a more macroscopic scale, i.e., on the lattice constant c, as shown in Fig. 1. As expected, due to the Possion effect, we observed the decreases of the c lattice constant with increasing in plane biaxial tensile strain. From Fig. 1(a) we obtained the ratio of the elastic constants ($2C_{13}/C + 33$) to be 0.99684, which is in good accordance with 1.0568 [24], 1.0165 [25], 1.0095 [26], and 0.91837 [27], experimentally and theoretically. The internal parameter u obviously shows a different strain behavior than the lattice constant c, it changes in the opposite way to the ratio of the lattice constants. The same behavior was also found in GaN and AlN under biaxial, uniaxial strains and hydrostatic pressure, which were related to the tendency of the wurtzite lattice to be resistant to changes of its bond length [28].

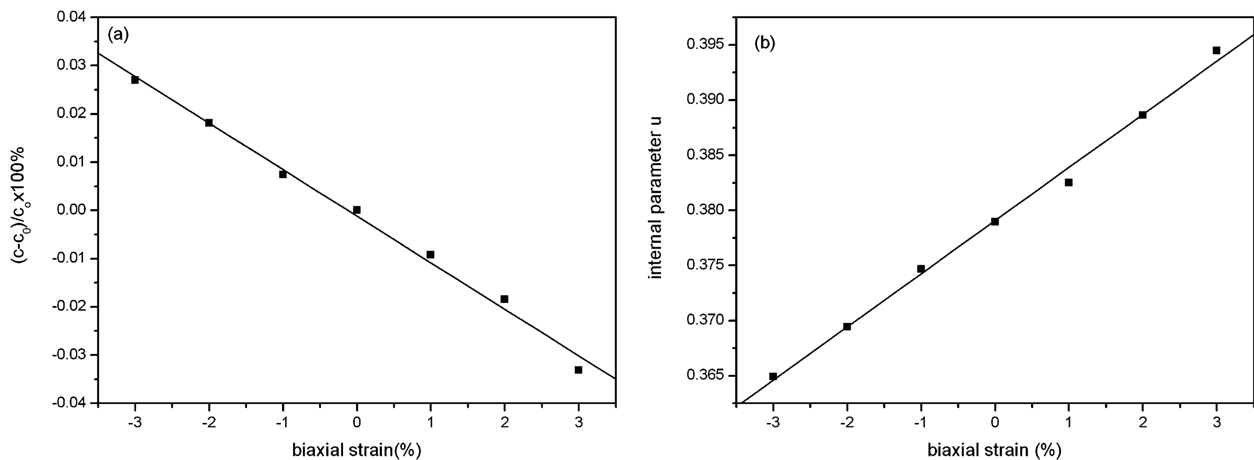

Fig. 1. The lattice constant c (a) and the internal parameter u (b) under in-plane biaxial strains.

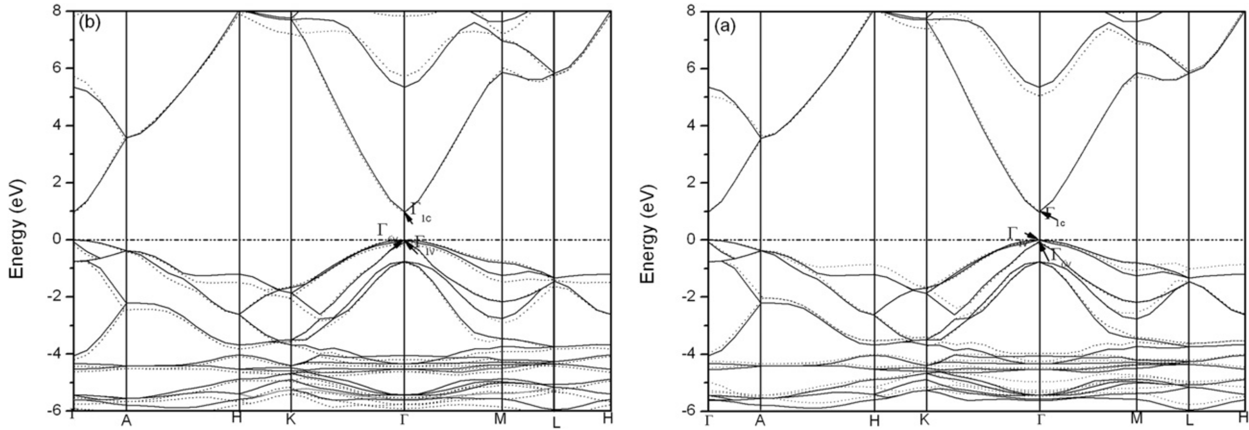

Fig. 2. Band structures of ZnO under strains of (a) +3% tensions and (b) −3% compressions compared with the unstrained one. The stone lines in both (a) and (b) represent the unstrained results.

The band structures are shown along high symmetry lines in hexagonal Brillion zone. Similar to the most binary semiconductors, the lowest conduction-band edge of ZnO originated from 4s states of atom Zn, whereas the states at the VBM from the 2p states of atom O. Both the VBM and the CBM occur at the Γ point $k = 0$ indicating that ZnO is a direct band gap semiconductor. We focused mainly on the uppermost of valence band as it is related to the holes in semiconductors. As spin-orbit coupling and spin degrees of freedom are neglected in our calculation, at the VBM the hexagonal crystal field Δ_{cf} splits the threefold-degenerate p level into a nondegenerate state and a doubly degenerate state in the standard notation denoted as Γ_1 and Γ_6, separated by 81 meV higher than the value 39.1 meV obtained by W.J. Fan et al., using EPM [29]. The fundamental band gap ($E(\Gamma_{1c})$–$E(\Gamma_{1v})$) is largely underestimated in GGA calculations, which has recently been overcome by the introduction of so-called self-interaction-corrected pseudopotentials [30]. We note that our calculation has overestimated the Δ_{cf}, it might be because of the underestimate of the fundamental gap increases the repulsive coupling between the Γ_{1v} valence and Γ_{1c} conduction band states. The residual strains influence both the energy gap E_g and the crystal-field splitting Δ_{cf} by the formulas described in Ref. [23]. Fig. 2 shows the band structures of ZnO under 3% in-plane tensile strain (a) and compressive strain (b), compared with the unstrained one (stone lines). We observed that for the compressed ZnO, the increased overlap between the orbital in the basal plane led to an overall broadening of the bands in the upper of the conduction bands and lower of the valence bands, but the bands near to the Fermi level come closer, thus provided a narrower band gap at the Γ point; on the contrary, the stretched strain resulted in the widening of the band gap. In Ref. [14], however, it showed that the band gap increases under both tensile and compressive strains, in contrast to the present results. These variations of E_g with strains are shown in Fig. 3. The energy gap varies nearly linearly with strains. This tendency is identical with the PL experiments of D.G. Zhao et al. [31] of the exciton spectra of wurtzite ZnO epilayers growing on various substrates. Additionally, the splitting energy of the crystal field Δ_{cf} decreases with the magnitude of the tensile strain, but increases with the

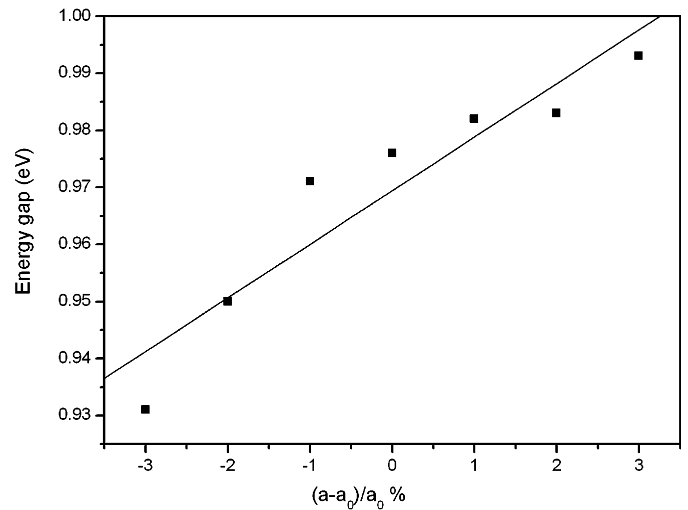

Fig. 3. The energy gap at Γ point of ZnO as the function of the in-plane biaxial strain.

compressive one, as shown in Fig. 4. Our results differ from GaN band structure calculation based on the sp^3d^5–sp^3 empirical tight-binding model of B. Jogai [15], which showed that the $|\Gamma_{1v} - \Gamma_{5v}|$ increased with the magnitude of the strain regardless of whether the strain is tensile or compressive. From the band structures, we observed the conduction- and valence-band minima remains at the Γ point that is the strained ZnO is still a direct band gap semiconductor, in contrast to the results that the tensile strains turned α-GaN into an indirect band gap structure [14]. Quantitative comparisons with the PR data would require the inclusion of the spin–orbit interaction and its coupling with both the crystal field and the strain. These effects have not yet been included in the present work.

The spin–orbit interaction has not been included in our calculation, therefore we could not see the removal of the degeneracy of Γ_6 and other spin degenerated states. However we still find that the strained VBM are flatter than the unstrained one, indicating that they have larger effective hole masses, which would affect the transportation properties the p-type ZnO, as we know, misfit of lattice constants and thermal expansion coefficients, as well as defects including dopants would induce strains in the thin film.

3.2. Optical properties under strains

The optical properties of matters can be described by means of the transverse dielectric function $\varepsilon(\omega)$. The imaginary part $\varepsilon_2(\omega)$ could be calculated from the momentum matrix elements between the occupied and unoccupied wave functions within the selection rules, and the real part $\varepsilon_1(\omega)$ can be evaluated from imaginary part $\varepsilon_2(\omega)$ by Kramer–Kronig relationship. All the other optical constants, such as reflectivity $R(\omega)$, absorption coefficient $a(\omega)$, refractive index $n(\omega)$, and energy-loss spectrum $L(\omega)$ can be derived from $\varepsilon_1(\omega)$ and $\varepsilon_2(\omega)$ [8].

Fig. 5 showed the imaginary part of the dielectric function $\varepsilon_2(\omega)$ of strained ZnO with the polarization along (a) and normal to (b) the c-axis, compared with the unstrained ZnO, the insets are the experimental results of unstrained ones [32]. As can be seen in these figures there is a close match between our calculated results and the experiment ones in the higher energy region (5–30 eV), and the compressive strains make the high energy peaks shift towards higher energy, which is the same with ZnO under hydrostatic pressures [8]. For lower energies considering the absorption edge of the spectra, the locations of the edge do not coincide. Therefore, we have shifted the edge upwards by a scissor of 2.37 eV; our calculated results give a good reproduction of spectra in the low energy region. Fig. 5(a) and (b) showed the anisotropy of the optical properties, and in-plane strain affected case (a) much apparently. The tensile strain push the peak around 13.5 eV higher, which mainly corresponded to the transition between the Zn 3d and O 2s states. The compressive strain shifted the peak around 8 eV upwards and made the appearance of the peak located at about 11 eV. The results for the dispersive part of the dielectric function $\varepsilon_1(\omega)$ of the ZnO polycrystalline are given in Fig. 6, the inset is the experimental results [33]. The main features in our calculated unstrained ZnO are: a peak at around 3 eV; another two lower peaks located at about 7 and 11 eV; a rather steep decrease between 11 and 17 eV, inside of which $\varepsilon_1(\omega)$ decreased toward zero then becomes negative finally reached a minimum; and then again a

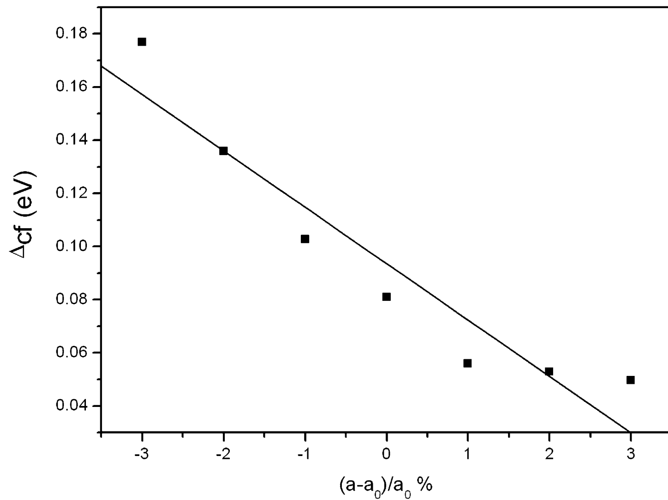

Fig. 4. The crystal field splitting energy Δ_{cf} as a of biaxial strains in the plane perpendi-cular to the hexagonal c-axis.

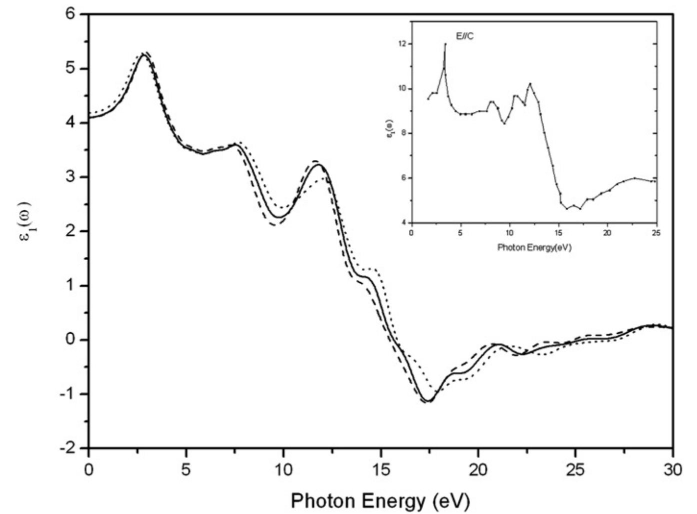

Fig. 6. The real part of dielectric function $\varepsilon_1(\omega)$ of the ZnO polycrystalline under strains. The inset is the experimental result.

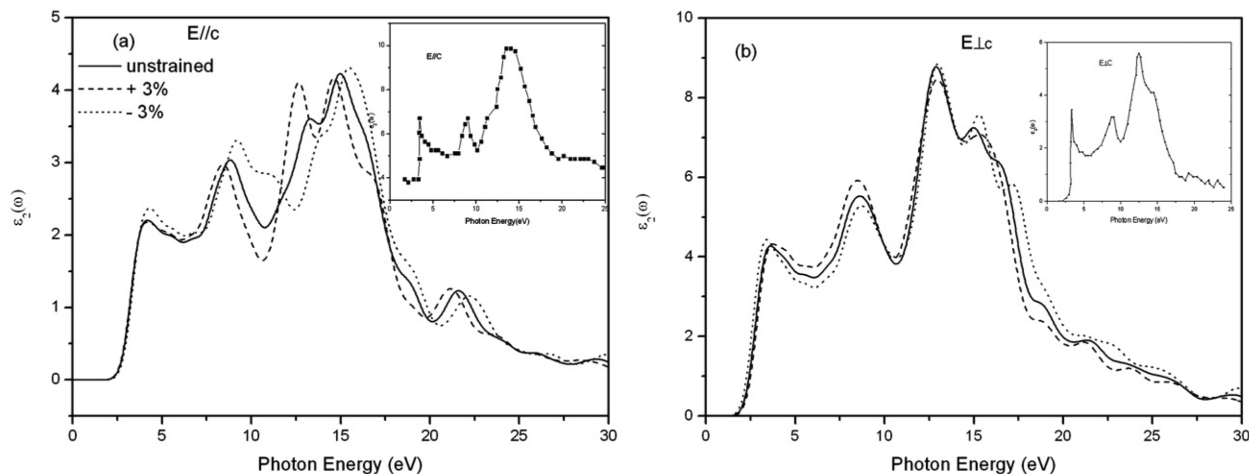

Fig. 5. The imaginary part of the dielectric function $\varepsilon(\omega)$ of the wurtzite ZnO thin film (a) polarization alone the c-axis (b) polarization in the ab plane. The inserts are the results of the experiments.

slow increase toward zero at higher energies. The strains make both the shape and the position of the main peaks of $\varepsilon_1(\omega)$ vary successively.

4. Conclusions

In conclusion, the electronic and optical properties of thin ZnO film under various residual in-plane biaxial strains were investigated by ab initio ultrasoft pseudopotential density functional method in details. From the strained band structures compared with unstrained one, we draw a conclusion that residual strains do affect the carrier transportation properties of p-type ZnO. The results of optical properties indicated that the residual strains affected the optical properties ZnO anisotropy and have remarkable characters at the high-energy regions. Therefore it is of great importance for understanding the strain influence on the properties of ZnO, especially the p-type one, as dopants induced large strain around them.

Acknowledgements

This work is supported by the Key Project of National Natural Science Foundation of China under Grant Nos. 60336020 and 50532050, the "973" program under Grant No. 2006CB604906, the Innovation Project of Chinese Academy of Sciences, and the National Natural Science Foundation of China under Grant Nos. 60429403, 60506014 and 10674133.

References

[1] D.C. Look, Mater. Sci. Eng. B 80 (2001) 383.
[2] D.M. Bagall, Y.F. Chen, Z. Zhu, T. Yao, S. Koyama, M.Y. Shen, T. Goto, Appl. Phys. Lett. 70 (1997) 2230.
[3] Y. Chen, D.M. Bagnall, H.-J. Koh, K.-T. Park, K. Hiraga, Z.-Q. Zhu, T. Yao, J. Appl. Phys. 84 (1998) 3912.
[4] M.A.L. Johnson, S. Fujita, W.H. Rowland Jr., W.C. Hughes, J.W. Cook Jr., J.F. Schetzina, J. Electron. Mater. 21 (1992) 157.
[5] R.J. Lad, P.D. Funkenbusch, C.R. Aita, J. Vac. Sci. Technol. 17 (1980) 808.
[6] D. Hwang, K. Bang, M. Jeong, J. Myoung, J. Cryst. Growth 254 (2003) 449.
[7] A. Ohtomo, K. Tamura, K. Saikusa, K. Takahashi, T. Makino, Y. Segawa, H. Koinuma, M. Kawasaki, Appl. Phys. Lett. 75 (1999) 2635.
[8] J. Sun, H.T. Wang, J.L. He, Y.J. Tian, Phys. Rev. B 71 (2005) 125132.
[9] M. Sanati, G.L.W. Hart, A. Zunger, Phys. Rev. B 68 (2003) 155210.
[10] A. Alan Porporati, Y. Tanaka, A. Matsutani, W. Zhu, G. Pezzotti, J. Appl. Phys. 100 (2006) 083515.
[11] D.G. Zhao, S.J. Xu, M.H. Xie, S.Y. Tong, Appl. Phys. Lett. 83 (2003) 677.
[12] J.-M. Wagner, F. Bechstedt, Phys. Rev. B 66 (2002) 115202.
[13] V. Timon, S. Brand, S.J. Clark, R.A. Abram, J. Phys.: Condens. Matter 16 (2004) 531.
[14] Z.Q. Yang, Z.Z. Xu, Phys. Rev. B 54 (1996) 17577.
[15] B. Jogai, Phys. Rev. B 57 (1998) 2382.
[16] R. Ghosh, D. Basak, S. Fujihara, J. Appl. Phys. 96 (2004) 2689.
[17] A.B.M.A. Ashrafi, N.T. Binh, B.P. Zhang, Y. Segawa, Appl. Phys. Lett. 84 (2004) 2814.
[18] M. Segall, P. Lindan, M. Probert, C. Pickard, P. Hasnip, S. Clark, M. Payne, J. Phys.: Condens. Matter 14 (2002) 2717.
[19] J.E. Jaffe, J.A. Snyder, Z. Lin, A.C. Hess, Phys. Rev. B 62 (2000) 1660.
[20] X. Zhu, S.G. Louie, Phys. Rev. B 43 (1991) 14142.
[21] D. Vanderbilt, Phys. Rev. B 41 (1990) 7892.
[22] J.S. Lin, A. Qteish, M.C. Payne, V. Heine, Phys. Rev. B 47 (1993) 4174.
[23] J.M. Wagner, F. Bechstedt, Phys. Rev. B 66 (2002) 115202.
[24] Z.C. Tu, X. Hu, Phys. Rev. B 74 (2006) 035434.
[25] X. Wu, D. Vanderbilt, D.R. Hamann, Phys. Rev. B 72 (2005) 035105.
[26] I.B. Kobiakov, Solid State Commun. 35 (1980) 305.
[27] T. Azuhata, M. Takesada, T. Yagi, A. Shikanai, S.F. Chichibu, K. Torii, A. Nakanura, T. Sota, G. Cantwell, D.B. Eason, C.W. Litton, J. Appl. Phys. 94 (2003) 968.
[28] A.F. Wright, J. Appl. Phys. 82 (1997) 2833.
[29] W.J. Fan, J.B. Xia, P.A. Agus, S.T. Tan, S.F. Yu, X.W. Sun, J. Appl. Phys. 99 (2006) 013702.
[30] D. Vogel, P. Kruger, J. Pollmann, Phys. Rev. B 54 (1996) 5495.
[31] D.G. Zhao, S.J. Xu, M.H. Xie, S.Y. Tong, H. Yang, Appl. Phys. Lett. 83 (2003) 677.
[32] J.L. Freeouf, Phys. Rev. B 7 (8) (1973) 3810.
[33] H. Yoshikawa, S. Adachi, Jpn. J. Appl. Phys. 36 (1) (1997) 6237.